



Research papers

Isotopic and spectral signatures unravel the sources, preservation and degradation of sedimentary organic matter in the Dongzhai Harbor mangrove estuary, southern China



Lu Yan ^{a,b}, Xianjun Xie ^{a,b,*}, James W. Heiss ^c, Kang Peng ^{a,b}, Yamin Deng ^{a,b}, Yiqun Gan ^{a,b}, Qinghua Li ^d, Yanpeng Zhang ^d

^a State Key Laboratory of Biogeology and Environmental Geology, School of Environmental Studies, China University of Geosciences, 430074 Wuhan, China

^b State Environmental Protection Key Laboratory of Source Apportionment and Control of Aquatic Pollution, Ministry of Ecology and Environment, 430074 Wuhan, China

^c Department of Environmental, Earth and Atmospheric Sciences, University of Massachusetts Lowell, Lowell, USA

^d Wuhan Center of China Geological Survey, Wuhan 430205, China

ARTICLE INFO

This manuscript was handled by Huaming Guo, Editor-in-Chief

Keywords:
Organic matter
Preservation
Isotope
Mangrove
Estuary
Aquaculture

ABSTRACT

Sedimentary organic matter (SOM) production and transformation processes have a prominent role in regulating biogenic element cycling in mangrove ecosystems. However, aquaculture biodeposits can substantially affect source apportionments and biogeochemical processes of SOM within mangroves. In this study, natural stable isotopes (^{13}C and ^{15}N), spectral techniques, and hydrogeochemical analysis were used to elucidate the sources, preservation, and degradation of SOM across the Dongzhai Harbor (DZH) estuary, southern China, where aquaculture systems are extensive. Along the estuarine salinity gradient, sediment and bottom water samples were collected from the upper fluvial mangrove zones to the lower marine endmember. Results indicated that source contributions to SOM along the estuarine gradient were spatially heterogeneous. Aquaculture-derived organic matter was the largest contributor to the Sanjiang River (44.29 %) in the upper estuary, and terrestrial sources from C3 mangrove forests were highest in the Yanfeng East River (62.87 %) near the middle estuary. Farther seaward, marine plankton sources were elevated in the Dongzhai Harbor channel (64.15 %) and Yanfeng West River (48.83 %) of the lower estuary. The terrestrial/microbial humic-like component (C1), tryptophan-like component (C2), and soil-derived fulvic acid (C3) were identified from the samples using fluorescence excitation emission matrices and parallel factor analysis (EEM-PARAFAC). Results show that in the upper and middle estuary, SOM was preserved by sedimentation due to the abundance of fine-grained aquaculture-derived biodeposits, weak hydrodynamic conditions, and the formation of Fe/Mn-humus complexes. In contrast, in the lower estuary, SOM originated from marine plankton and was rapidly degraded via aerobic respiration. Moreover, correlations between $\delta^{13}\text{C}$ and $\delta^{15}\text{N}$ values vs C/N ratios further suggest progressive SOM degradation from initial diagenesis to post-depositional geochemical processes. This study provides new insights into aquacultural and environmental factors controlling SOM preservation and degradation within estuaries. The findings have implications for shoreline stability and the protection and restoration of estuarine mangrove wetlands.

1. Introduction

Benthic sediments serve as sources and sinks of organic matter (OM), playing a pivotal role in controlling global biogeochemical cycling of sedimentary organic matter (SOM) and biogenic elements (Schartup et al., 2014). Estuarine SOM can have multiple sources, including

allochthonous inputs (e.g., soil/plant materials and waste discharge) (Bauer et al., 2013) and autochthonous production (e.g., *in situ* marine plankton-derived substances) (Samantaray and Sanyal, 2022). Furthermore, over 90 % of SOM can be trapped and preserved in sediments through incorporation into Fe/Mn-(hydr)oxide and clay minerals, which can reduce the bioavailability of SOM in environments where redox

* Corresponding author at: State Key Laboratory of Biogeology and Environmental Geology, School of Environmental Studies, China University of Geosciences, 430074 Wuhan, China.

E-mail address: xjxie@cug.edu.cn (X. Xie).

conditions oscillate (Conant et al., 2011; Chen et al., 2018). Depending on the depositional environment and the nature of SOM, the quantity and quality of buried SOM can vary considerably (Resmi et al. 2016). Consequently, owing largely to the coupled influence of marine and terrestrial sources, SOM in mangrove estuaries is compositionally complex and often exhibits varying degrees of reactivity.

Microbial processing of SOM is a chemically important process that affects elemental cycling and mangrove health in the coastal zone. Mangroves thrive in land–ocean transition zones where there are high levels of sediment deposition, an abundance of organic-rich deposits, and where anoxic conditions persist (Alongi, 2014; Deborde et al., 2015; Wang et al., 2019). Nevertheless, hydrodynamic (e.g., tide, typhoon, storm surge and sea level rise) and anthropogenic (e.g., aquaculture, agriculture, and urbanization) pressures are causing mangroves to disappear at an alarming rate (Marchand et al., 2011). Typically, wastes produced by marine aquaculture increase SOM deposition rates by one or two orders of magnitude above natural background levels, and also act as nutrient and energy sources for microbes (Martinez-Garcia et al., 2015). Benthic environments with low oxygen levels motivate anaerobic metabolic pathways, primarily sulfate reduction, Fe/Mn respiration, and methanogenesis, leading to SOM degradation processes (Kappler et al., 2021). Moreover, several microbial metabolites, such as sulfide (H_2S), reduced iron (FeS), trace elements and organic acids produced in hypoxia conditions, are toxic to mangrove forests (Alongi, 2021). Therefore, knowledge of the sources and processes impacting the SOM preservation and degradation is essential to understand the transport and transformations of biogenic elements, which ultimately regulate the health of coastal mangrove wetland environments.

Analysis of stable isotopic compositions (^{13}C and ^{15}N) and mixing models are effective methods for estimating SOM sources and degradation processes (Derrien et al., 2019). In addition, fluorescence spectroscopy, excitation-emission matrix (EEM) coupled with parallel factor analysis (PARAFAC) have been successfully applied to characterize SOM sources and dynamics in coastal ecosystems (Chen and Hur, 2015; Qiao et al., 2021; Zhang et al., 2021). Fluorescent OM is primarily composed of humic substances that are preferentially preserved in sediments under anoxic conditions, while other components are readily metabolized by heterotrophic bacteria such as aromatic amino acids/proteins (Chen and Jaffe, 2014).

Dongzhai Harbor (Hainan Island, China) is the first mangrove nature reserve in China. As aquaculture and tourism have grown rapidly in the past six decades, the mangrove area has been significantly reduced from initial $\sim 40\text{ km}^2$ to 17 km^2 (He et al., 2019). High-level shrimp farming has caused eutrophication of mangrove wetland water bodies, further triggering the outbreak of wood boring isopod, *Sphaeroma* species (Xu et al., 2014). These wood borers attacked the mangroves species *Bru-guiera* spp. mostly, and followed by *Ceriops tagal*, *Avicennia marina*, *Kandelia obovata* and *Aegiceras corniculatum* (Thiri and Yang, 2022).

Most previous studies have analyzed elemental composition and stable carbon isotopes to characterize SOM in coastal zones, such as the Yangtze River Estuary (Zhou et al., 2022), Pearl River Delta (Dan et al., 2021), and Pichavaram estuary (Naidu et al., 2022). However, in complex mangrove estuaries with intensive aquacultural activities, the decomposition and burial processes of SOM has received little attention to date. Notably, the continuous supply of labile biodeposits from aquaculture ponds to benthic sediments may promote the remineralization of refractory SOM, which can affect biogenic element budgets in mangrove ecosystems (Santos et al., 2021). Therefore, the objectives of this study were to: (1) quantify the relative contribution of SOM from heterogeneous sources using $\delta^{13}C$ and $\delta^{15}N$ three-endmember mixing models; (2) identify key constraints on SOM preservation and degradation; and (3) characterize SOM biogeochemical processes that affect mangrove environments along estuarine salinity gradients.

2. Materials and methods

2.1. Study area and sampling

The Dongzhai Harbor (DZH) mangrove estuary, covering an area of $\sim 100\text{ km}^2$, is located in the northeastern part of Hainan Island, China (N $19^{\circ}51' - 20^{\circ}01'$, E $110^{\circ}30' - 110^{\circ}37'$) (Liu et al., 2019) and has an irregular semidiurnal tide. Averagely, there is 1.92 m tidal range during spring tides and 0.38 m during neap tides (Li et al., 2013). The estuary is funnel shaped and is connected to the Qiongzhou Strait to the north (Fig. 1). The mean annual rainfall in the region is 1676 mm , of which 80 % falls from May to October (Xiong et al., 2018). The mangrove in Dongzhai Harbor estuary occupy a $\sim 40\text{ km}^2$ area and are located in three distinct areas of the estuary: Sanjiang River (hereafter termed as the upstream river), Yanfeng East River (midstream river) and Yanfeng West River (downstream river) (Xia et al., 2021). Generally, the northeast side of the estuary is an alluvial floodplain consisting mainly of silty sand, sandy silt, and gravel. In contrast, the southwest region is primarily composed of Quaternary basalt and tuff with lateritic soils due to long-term weathering (Li et al., 2013). The estuary is bordered by tidal rivers and contains multiple shrimp and shellfish ponds that are raised above sea level. Aquaculture and densely populated areas are concentrated around Sanjiang River located in the southern part of Dongzhai Harbor.

In November 2019, 46 benthic sediment samples were collected from a depth interval of $0 - 10\text{ cm}$ below the bed using a stainless-steel Peterson grab sampler (Fig. 1). Samples were collected during a flooding tide stage by cruising together with several boats from the most downstream to upstream sampling sites. Three sets of sediment subsamples were then collected from each grab sample. The subsamples were mixed to obtain a representative sample of the sediment at each sampling site. At each sampling site, bottom water hydrochemical parameters including pH, salinity (S), EC, and dissolved oxygen (DO) were measured on site with a calibrated portable multimeter (model HQ40d, Hach Company). Sampling spanned the land-sea transition zone and included three large mangrove tidal rivers and within the Dongzhai Harbor channel, for a total of four areas (Fig. 1C). Thus, the sampling sites captured the full range of SOM characteristics within and surrounding the mangrove estuary and included areas near aquaculture ponds.

The samples were classified according to location along the land-sea gradient. Samples representing marine sediments are labeled S24-S40 (orange) in Fig. 1C. The sites labeled S1-S11 (blue), S12-S17 (purple) and S18-S23 (pink) are fluvial sites and are located in the downstream river, midstream river and upstream river, respectively. All samples were kept in self-sealing polyethylene bags and were frozen and stored at -20°C until analysis.

2.2. Laboratory analysis

2.2.1. Sediment geochemistry analysis

Samples for trace elemental measurements were air-dried and ground to 200 ($74\text{ }\mu\text{m}$) mesh. Approximately 0.5 g of sieved sample was digested in a mixture of concentrated HNO_3 (9 ml), HCl (2 ml), and HF (3 ml) at 108°C in an oven for 24 h, evaporated to dryness. 50 ml of 2 % purified HNO_3 was then added to dilute the sample. Total Fe, Mn, P, and S were measured using inductively coupled plasma mass spectrometry (ICP-MS) (Element II, Thermo-Fisher). The analytical precision of the instrument was $\pm 8\text{ %}$.

Grain size was quantified with a laser particle size analyzer (Mastersizer 3000, Malvern Instrument Ltd., UK). Sediment samples were pretreated prior to grain size analysis according to the methods described by Gu et al. (2016), whereby grain size was characterized into three groups: clay ($<4.0\text{ }\mu\text{m}$), silt ($4.0 - 63.0\text{ }\mu\text{m}$) and sand ($>63.0\text{ }\mu\text{m}$) (Wentworth, 1922). The analytical precision of the particle size analyzer was $<2\text{ %}$.

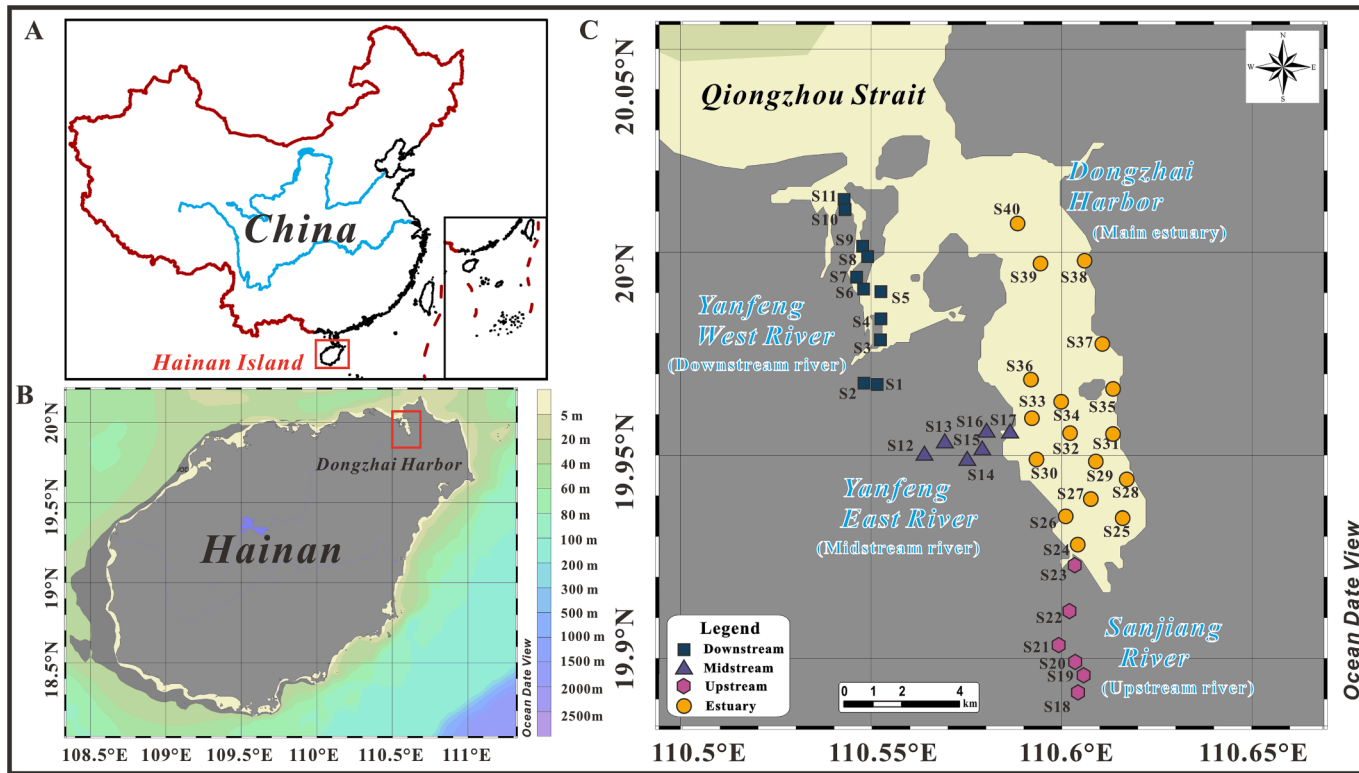


Fig. 1. Regional maps of the Dongzhai Harbor estuary (A & B), and sampling site locations in the Dongzhai Harbor channel (main estuary) and three rivers (C).

2.2.2. TOC, TN, $\delta^{13}\text{C}$ and $\delta^{15}\text{N}$ analysis

C/N ratios and $\delta^{13}\text{C}$ and $\delta^{15}\text{N}$ values can be used to characterize the origin and transformation of SOM in coastal ecosystems (Tesi et al., 2008). Analysis of total organic carbon (TOC), total nitrogen (TN), $\delta^{13}\text{C}$, and $\delta^{15}\text{N}$ analyses followed the procedures of Gu et al. (2017). For TOC and TN, 40–50 mg of pretreated dry sediments were placed into tin capsules before being placed in a vario PYRO cube elemental analyzer (Elementar, Germany) with an auto sampler. Replicate analysis on each sample showed that the measurement precision for TOC and TN was <1 %. Measurements of $\delta^{13}\text{C}$ and $\delta^{15}\text{N}$ isotopic values were conducted with an IsoPrime100 isotope ratio mass spectrometer (Isoprime, Britain). The results herein are expressed as per thousand (‰), calculated as follows:

$$\delta^{13}\text{Cor} \delta^{15}\text{N} (\text{\textperthousand}) = (R_{\text{sample}} / R_{\text{reference}} - 1) \times 1000$$

where R_{sample} and $R_{\text{reference}}$ are the isotopic ratios of the sample and reference, respectively. $\delta^{13}\text{C}$ was calibrated with the Vienna PeeDee Belemnite (PDB) standard USGS24 and IAEA600 ($\delta^{13}\text{C}_{\text{PDB}} = -27.5 \text{ ‰}$), while $\delta^{15}\text{N}$ was corrected using the atmospheric air standard IAEA N₁ and USGS43 ($\delta^{15}\text{N}_{\text{air}} = 0.4 \text{ ‰}$). The analytical precision was <0.1 ‰ for both $\delta^{13}\text{C}$ and $\delta^{15}\text{N}$.

2.2.3. Fluorescence analysis of SOM

The fraction of water-extractable organic matter (WEOM) has been used previously to identify land-based soil OM (Zsolnay, 2003; Huang et al., 2015). We followed the approach of He et al. (2013) to quantify WEOM. 2.0 g of sediment was extracted using 10 ml milli-Q water (solid to water ratio of 1:5, w/v) in a centrifuge tube. After shaking for 16 h at 130 rpm, the suspension was centrifuged at 10,000 rpm for 15 min and filtered through Whatman GF/F (0.45 μm) membranes. The filtrates were then stored in the dark at <4 °C until fluorescence analysis.

EEM spectra (EEMs) analysis was performed on an F-4600 fluorescence spectrometer (Hitachi High Technologies, Tokyo, Japan) with a 1-cm quartz cell at room temperature. The excitation (Ex) wavelength was set from 200 to 450 nm (5 nm intervals), while the emission (Em) spectra

ranged from 250 to 600 nm (2 nm intervals). Additionally, the slit widths for both Ex and Em monochromators were set at 5 nm, and the scan speed was adjusted to 12,000 nm min⁻¹. To reduce inner-filter effects, the EEMs were corrected for absorbance by multiplying each EEMs value with a correction factor (Burdige et al., 2004). Milli-Q water EEMs was subtracted to eliminate the first- and second-order Rayleigh and Raman scattering from each sample. The integrated area of the Raman peak (Ex = 350 nm) was calculated using Milli-Q as a reference (Gan et al., 2020). PARAFAC modeling of EEMs was used to identify the fluorescent components of WEOM, which was conducted according to Stedmon and Bro (2008). To characterize WEOM properties, two spectroscopic indices, humification index (HIX) and biological index (BIX), were calculated from the EEMs.

$$\text{HIX} = \frac{\sum F_{\text{Em}=435-480}}{\sum F_{\text{Em}=300-345}}, \lambda_{\text{Ex}} = 254 \text{ nm}$$

$$\text{BIX} = \frac{F_{380}}{F_{430}}, \lambda_{\text{Ex}} = 310 \text{ nm}$$

2.3. TEMM model based on Monte Carlo simulations of isotope ratios

Bayesian Markov chain Monte Carlo (MCMC) approach was applied to quantify the relative contributions of potential sources to SOM (Andersson, 2011; Bosch et al., 2015; Li et al., 2020b). The MCMC computations produced 100 million normally distributed random numbers based on an $\delta^{13}\text{C}$ and $\delta^{15}\text{N}$ three-endmember mixing (TEMM) model. One million of these values were then used to estimate the proportions of SOM sources (Li et al., 2020c). Statistical parameters (e.g., mean, median, maximum, minimum, and standard deviation) were computed from the TEMM model. The ^{13}C - ^{15}N isotopic mixing equations are as follows:

$$\left(\frac{^{13}\text{C}}{^{12}\text{C}} \right)_{\text{mixture}} = \sum_{i=1}^n x_i K_i^C \left(\frac{^{13}\text{C}}{^{12}\text{C}} \right)_i / \sum_{i=1}^n x_i K_i^C$$

$$\left(\frac{^{15}\text{N}}{^{14}\text{N}}\right)_{mixture} = \sum_{i=1}^n x_i K_i^N \left(\frac{^{15}\text{N}}{^{14}\text{N}}\right)_i / \sum_{i=1}^n x_i K_i^N$$

$$\sum_{i=1}^n x_i = 1$$

where n is the number of endmembers, K_i is the C or N concentration of source i , and x_i is the fractional sediment mass contribution of source i (Wang et al., 2021).

The $\delta^{13}\text{C}$ and $\delta^{15}\text{N}$ endmember values were selected by dividing the SOM samples into three pools: terrestrial, aquaculture, and marine. These pools make up the dominate land cover within and surrounding the estuary (Yan et al., 2021). The mean $\delta^{13}\text{C}$ and $\delta^{15}\text{N}$ values measured in the samples of each pool were defined as the end member. The $\delta^{13}\text{C}$ and $\delta^{15}\text{N}$ isotopic values of the terrestrial endmember were $-26.9 \pm 0.40 \text{ ‰}$ and $7.0 \pm 1.46 \text{ ‰}$, while those for the marine endmember were $-23.7 \pm 0.96 \text{ ‰}$ and $5.4 \pm 0.95 \text{ ‰}$, respectively. The benthic sediments in the upstream river were used to define the aquaculture endmember ($\delta^{13}\text{C}: -25.7 \pm 1.00 \text{ ‰}, \delta^{15}\text{N}: 4.9 \pm 0.28 \text{ ‰}$), because aquaculture ponds are extensive in the area.

2.4. Statistical analyses

The spatial distribution of sampling sites was mapped with Ocean Data View software (ODV Version 5.5.1) (Schlitzer, Reiner, Ocean Data View, <https://odv.awi.de>, 2021). The TEMM and PARAFAC modelling were performed in MATLAB R2015b (MathWorks, Inc., US). Statistical analyses including correlation analysis, t-tests, and principal components analysis (PCA) were performed with Origin 2018 software (Microcal Software, Inc., Northampton, MA). Statistically significant differences were evaluated at the $P < 0.05$ levels using the least significant differences (LSD).

3. Results

3.1. Hydrogeochemical properties

Bottom water salinity, pH, and DO were spatially variable along the land-sea gradient. The results of the statistical analysis of the hydrogeochemical parameters are presented in Table 1. In the DZH mangrove estuary, bottom water salinity ranged from 7.88 to 30.70 psu and the EC values varied from 14.74 to 51.60 ms/cm, indicating strong tidal mixing. The average salinity of the upstream river, midstream river,

Table 1
Hydrogeochemical properties of benthic sediments and bottom water samples collected from within the DZH estuary and its three tidal rivers.

	MIN.	MAX.	AVER.	S.D.
<i>Bottom water</i>				
Salinity (psu)	7.88	30.70	23.34	6.04
EC (ms/cm)	14.74	51.60	39.08	10.11
pH	7.00	8.07	7.63	0.29
DO (mg/L)	3.66	8.48	6.82	1.35
<i>Sediment</i>				
TOC (%)	0.09	4.09	0.85	0.88
TN (%)	0.02	0.30	0.09	0.06
C/N	4.07	13.44	7.66	2.36
$\delta^{15}\text{N}$	3.52	11.46	5.49	1.52
$\delta^{13}\text{C}$	-27.47	-21.79	-24.77	1.47
TP (µg/g)	110.00	1550.00	690.50	327.02
TS (%)	0.07	1.04	0.41	0.23
Fe ₂ O ₃ (mg/kg)	6.20	91.40	41.58	1.88
Mn (µg/g)	118.00	1840.00	468.78	337.59
Clay (%)	5.50	39.78	19.72	8.89
Silt (%)	10.68	60.09	38.01	14.28
Sand (%)	6.50	83.82	42.08	22.16

downstream river and main estuary were 13.00, 17.72, 28.29, 25.78 psu. pH and DO increased with salinity from headwaters to the estuary and ranged from 7.00 to 8.0 and from 3.66 to 8.48 mg/L, respectively.

The sediment biogenic elements (TOC, TN, TP, TS, Fe₂O₃ and Mn) and isotope values also exhibited considerable spatial variability (Fig. 2 & Fig. S1). Generally, the fluvial sediments contained more biogenic elements than marine sediments. The contents of TOC, TN, TP, TS, Fe₂O₃, and Mn in the midstream river were the highest with averages of 2.60 %, 0.22 %, 1235 µg/g, 0.77 %, 73.6 mg/kg, and 903.2 µg/g, respectively, followed by the upstream river (1.25 %, 0.13 %, 936.7 µg/g, 0.53 %, 58.6 mg/kg, and 530.0 µg/g). The average $\delta^{13}\text{C}$ value in the main estuary (-23.7 ‰) was higher compared to the downstream river (-24.8 ‰), upstream river (-25.7 ‰), and midstream river (-26.9 ‰). In contrast, the highest average $\delta^{15}\text{N}$ value was measured in the midstream (+6.99 ‰), followed by estuary (+5.38 ‰), downstream (+5.15 ‰), and upstream (+4.94 ‰).

3.2. Grain size distribution of sediments

A ternary diagram of the grain size distribution shows that surface sediments were composed primarily of silt and sand (Fig. S2). Only the upstream river, a section of the midstream river, and the upper region of the estuary comprised of more than 25 % clay (Fig. S2). Sediments in the upstream river and midstream river were mainly clayey silt and silty sand, while the downstream river was composed of coarser silty sand. In the DZH channel, proportions of fine-grained sediments decreased slightly from the upper estuary to near the mouth of the harbor, whereas the opposite trend was observed for coarse-silty-sand sediments (Table S1).

The spatial distributions of sediment grain size are depicted in Fig. S3. Generally, mean values of fine-grained sediments decreased from the upstream (71.16 %)/midstream river (61.94 %) to the downstream river (50.44 %)/estuary (56.22 %). On the contrary, sand fractions increased gradually up the salinity gradient, with mean values of 28.41 % (upstream), 37.32 % (midstream), 43.75 % (estuary) and 49.56 % (downstream), respectively. This distribution patterns of sediment texture may be attributed to dynamic diversion, a complex interaction between longshore currents and tidal flow. Similarly, near the Jiaozhou Bay mouth, sediment is even dominated by gravel, and a deep trough is formed there due to tidal current scouring (Hu et al., 2018).

Sediment grain size appeared to be impacted by aquaculture activities. Owing to riverine discharges, input of fecal pellets and pseudofeces from intensive shellfish culture can increase the abundance of fine-grained benthic sediments (Xu et al., 2020).

As shown in Fig. 3, there are significant positive relationships between biogenic elements and clay content. Because fecal pellets and pseudofeces increase clay content (Kennedy et al., 2014), the relationships suggest that input of OM from upstream shellfish cultures is an important control on SOM adsorption and elemental cycling in the tidal rivers. This finding is supported by previous studies which have shown that granular characteristics can affect the geochemical behavior of organic matter and biogenic elements in sedimentary environments (Martinez-Garcia et al., 2015).

3.3. Variations of TOC, TN, $\delta^{13}\text{C}$, $\delta^{15}\text{N}$ and elemental ratios

The correlation between TOC and TN was statistically significant ($p < 0.001$) (Fig. 4A), indicating a common source. Moreover, the fitting line intercept was close to zero (i.e., 0.03 %) suggesting that TN was predominantly organic nitrogen (Goñi et al., 2013). TOC content ranged from 0.09 % to 4.09 % (average 0.85 %), and TN ranged from 0.02 % to 0.30 % (average 0.09 %). The TOC and TN levels in the DZH mangrove estuary were within the range reported for other coastal estuaries affected by aquaculture, such as the Africa Cross River estuary (Dan et al., 2019), Rufiji Delta (Minu et al., 2020), Maowei Sea (Xu et al., 2020) and Qinglan Harbor (Bao et al., 2013). Mangrove estuaries

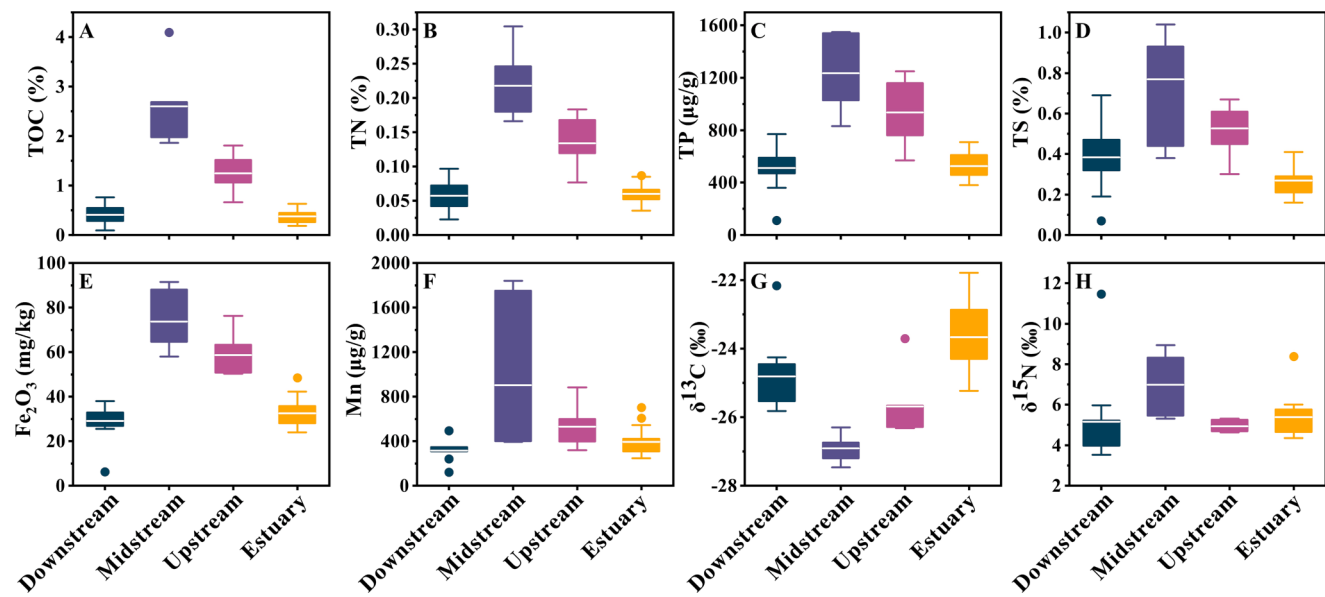


Fig. 2. Box plots of biogenic element content and $\delta^{13}\text{C}$ and $\delta^{15}\text{N}$ values measured in samples collected in the fluvial and marine sediments. The top and bottom of the boxes illustrate the 25th and 75th percentiles and the solid white line within the box indicates the mean. Whiskers extend from the box to observations with values within 1.5 times the inner-quartile range of the box, with dots as outliers.

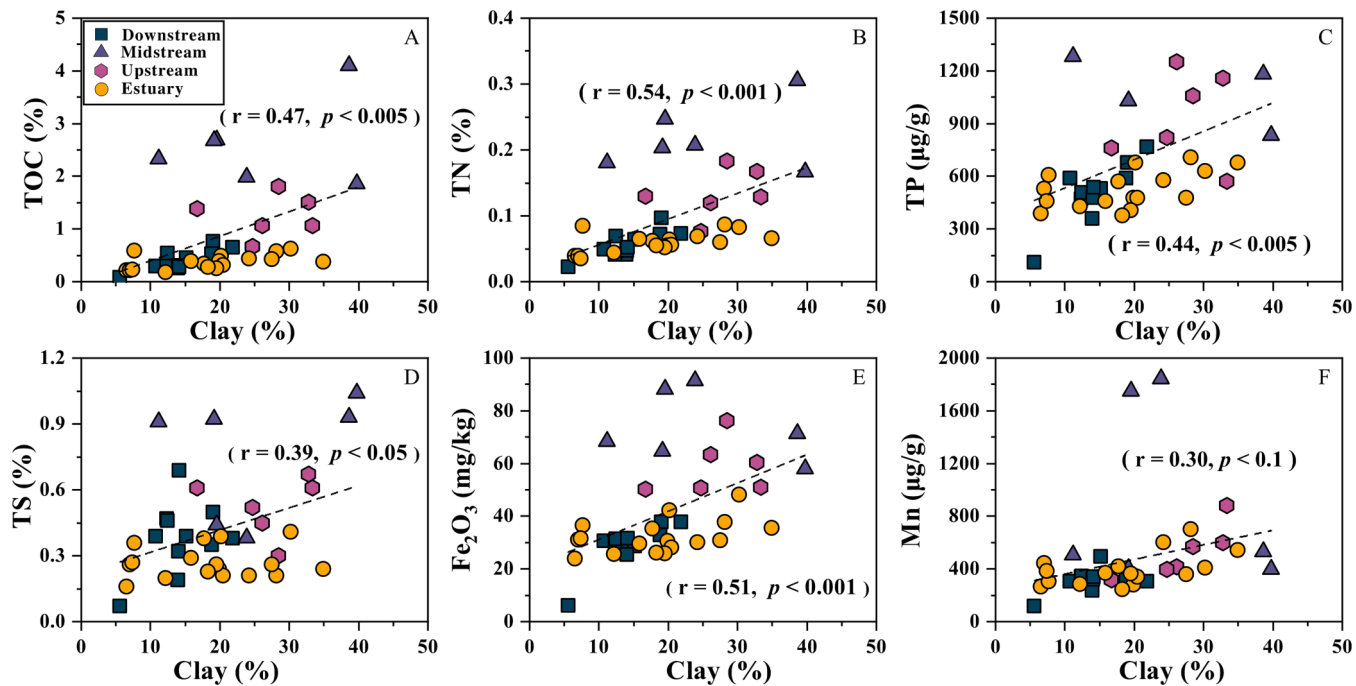


Fig. 3. Correlations between biogenic elements and clay content in surface sediments of the DZH estuary.

without aquaculture have lower TOC and TN values than found in the DZH estuary, such as Conception Bay (Marchand et al., 2011), Bangladesh Sundarban (Prasad et al., 2017) and the Rio Caeté estuary (Koch et al., 2011). These results suggest that SOM in estuaries is strongly influenced by the intensity of nearby aquaculture activities.

C/N ratios and $\delta^{13}\text{C}$ and $\delta^{15}\text{N}$ values of all samples ranged from 4.07 to 13.44 (C/N), -27.47 ‰ to -21.79 ‰ ($\delta^{13}\text{C}$), and 3.52 ‰ to 11.46 ‰ ($\delta^{15}\text{N}$) (Table 1). Typically, terrestrial vascular plants have relatively high C/N ratios (>12) because vegetative material is composed of lignin and cellulose, which are nitrogen poor (Lamb et al., 2006). C/N ratios of marine plankton tend to be lower; studies have shown ratios to range from 4 to 10, with an average between 5 and 7 (Kirkby et al., 2011). In

this study, the average C/N ratio (7.66) was similar to the ratios in abalone culture areas of Ailian Bay (C/N: 7.46) (Pan et al., 2019) and Zhelin Bay (C/N: 7.31) (Gu et al., 2017), which have been heavily impacted by aquaculture activities. The relationship between $\delta^{13}\text{C}$ and C/N was negative, while the relationship between $\delta^{15}\text{N}$ and C/N was positive, and both correlations were statistically significant (Fig. 4B & 4C). Additionally, C/N ratios and $\delta^{15}\text{N}$ composition gradually decreased from the upper estuary to the lower estuary. These results imply that sedimentary organic matter in the upstream regions (upstream river & midstream river) received higher contributions from terrigenous sources relative to the downstream regions (downstream river & main estuary).

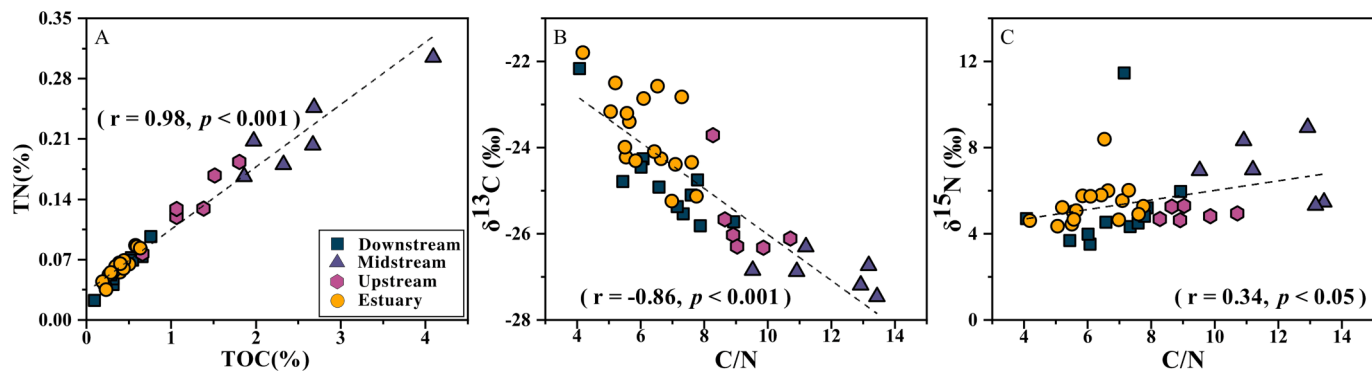


Fig. 4. Relationships between A) TOC and TN, B) $\delta^{13}\text{C}$ and C/N, C) $\delta^{15}\text{N}$ and C/N in benthic sediments of the DZH estuary.

3.4. Optical characteristics of SOM

Three fluorescent components (C1-C3) of SOM were identified using PARAFAC modeling (Fig. 5). The C1 (Ex/Em maxima: (235)340/440 nm) component has been assigned as peak C and identified as terrestrial (allochthonous) humic-like material (Coble et al., 1998; Li et al., 2020a). In some cases, C1-like components were considered as microbial degraded/diagenetic products of organic matter (Yamashita et al., 2010; Du et al., 2021). C2 (Ex/Em maxima: (<250)320/390 nm) was consistent with the fluorescence spectra of coalescing M and T peaks and was surmised as originating from marine humic-like or tryptophan-like materials. Typically, this component was found in proteinaceous substances from fresh (autochthonous) organic matter (Clark et al., 2008). The C3 (Ex/Em maxima: 395/500 nm) component closely resembled soil-derived fulvic acid (Osburn et al., 2016), while peaks of similar fluorescent spectra have not been well defined in recent studies.

In general, the relative intensity of C1 (%C1) was the highest, ranging from 51.58 to 76.83 %, followed by C3 (15.46–33.14 %) and C2 (3.82–22.58 %). Slightly higher HIX values were observed in the midstream sediments (1.27–4.10) than in other three regions (upstream:

0.94–2.59; downstream: 0.99–2.31; main estuary: 0.88–2.64) (Table S3), indicating a higher degree of SOM humification and abundance of refractory substances in the middle estuary (Guo et al., 2019). The BIX values were similar across all sample sites, ranging from 0.51 to 0.74 (average: 0.62), while the upstream sediment samples had relatively higher BIX values (average: 0.66) (Table S3), which suggests SOM source contributions from aquaculture biodeposition (Yang et al., 2014).

4. Discussion

4.1. Relative source contributions of SOM based on $\delta^{13}\text{C}$ and $\delta^{15}\text{N}$ three-endmember mixing model

Spatial heterogeneity was observed in SOM source apportionments of fluvial and marine sediments. The $\delta^{13}\text{C}$ and $\delta^{15}\text{N}$ values were used in a three-endmember mixing model to quantify the relative contributions of SOM from the three potential sources (terrestrial OM, aquaculture-derived OM, and marine plankton OM). Table S2 and Fig. 6B show the Monte Carlo model results of the proportional source contributions of SOM. In fluvial sediments (upstream river, midstream river, &

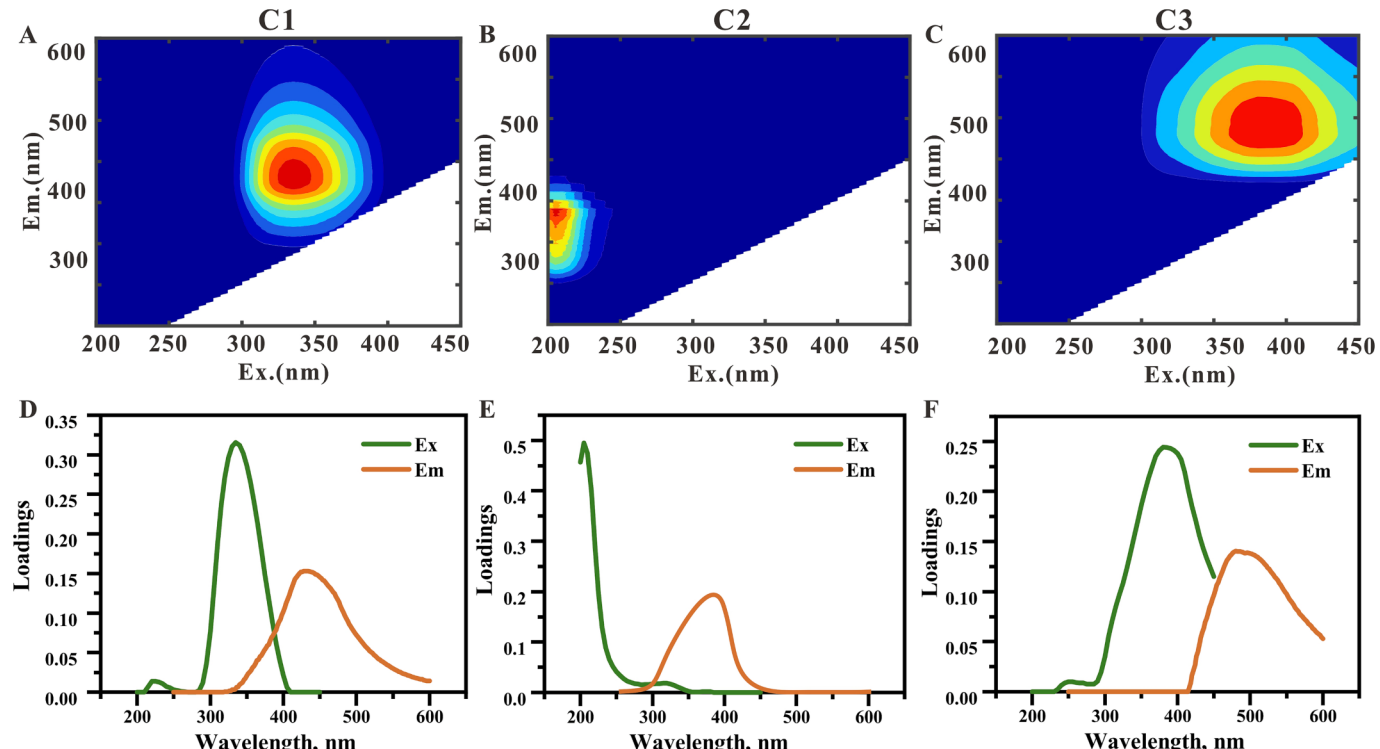


Fig. 5. Three DOM components identified using PARAFAC modeling.

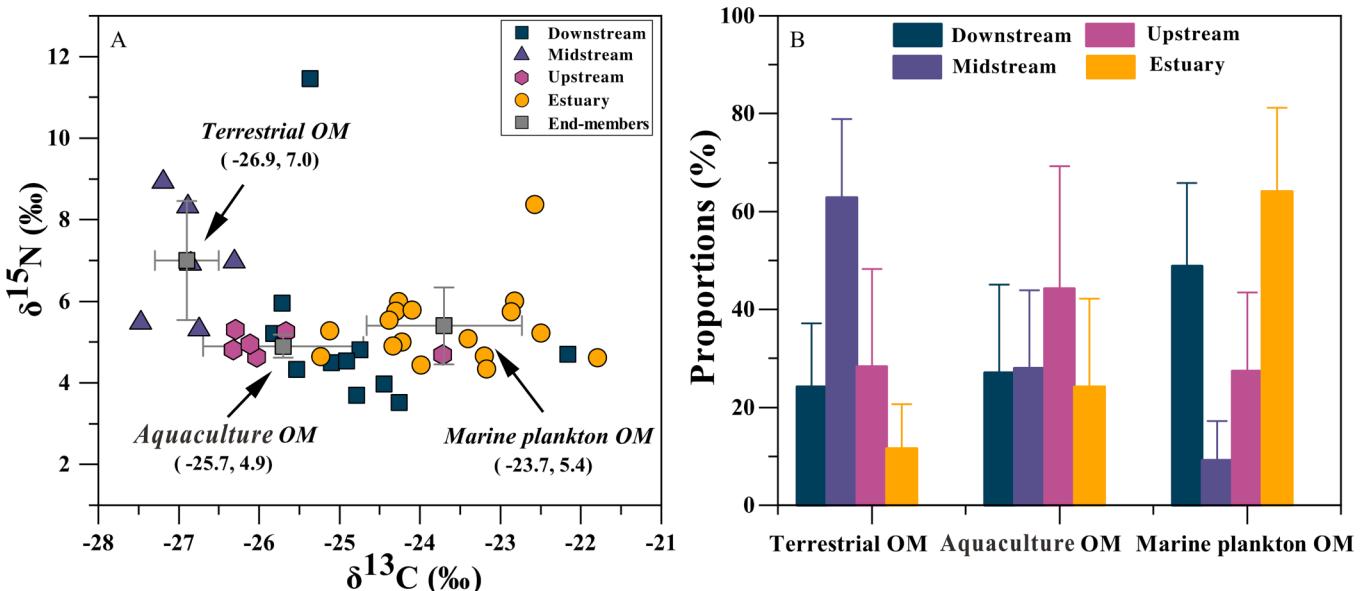


Fig. 6. A) Stable organic carbon and nitrogen isotope signatures ($\delta^{13}\text{C}$ vs $\delta^{15}\text{N}$) and B) their potential source contributions to SOM in the DZH mangrove estuary.

downstream river), organic matter was mainly derived from terrestrial sources (mean: 35.33 %), while planktonic OM (mean: 63.99 %) was the dominant source of SOM in marine benthic sediment (main estuary). On average, the proportion of SOM originating from terrestrial aquaculture ponds was higher in fluvial sediments (31.76 %) compared to marine sediments (22.98 %). These results indicate that aquaculture activities had a large impact on SOM source, and that this effect diminished with increasing distance from aquaculture regions.

The upstream river, draining into the upper estuary, received the largest proportion of aquaculture-derived organic matter (44.29 %), followed by the midstream river (27.93 %), downstream river (27.02 %) and main estuary (24.23 %). Further, the mean $\delta^{15}\text{N}$ composition of SOM in the upstream river was $4.94 \pm 0.28\text{ ‰}$ (Fig. 6A), which is similar to the $\delta^{15}\text{N}$ composition of shellfish fecal matter biodeposits in Ailian Bay ($5.12 \pm 0.20\text{ ‰}$) (Pan et al., 2019). Both our $\delta^{15}\text{N}$ composition values for the upstream river and the values from Ailian Bay are lower than anthropogenic sewage (10 % to 25 %), which tends to be isotopically rich in heavy nitrogenous components (Fenech et al., 2012). Thus, our lower observed $\delta^{15}\text{N}$ values in the upstream river were likely due to fecal matter inputs derived from aquaculture. The results are consistent with the high population density along the upstream river as well as the prevalence of aquaculture ponds and wastewater discharge in the area. These anthropogenic influences increased organic matter and biogenic elements accumulation and burial in the upstream river. The composition and sources of SOM are also affected by controls of surface water hydrodynamics on suspended particulate organic matter production rates. Sarà et al. (2004) and Ayvazian et al. (2021) found that weak tidal currents increased particulate organic matter production, leading to higher levels of SOM. These findings suggest that fecal matter sourced from aquaculture ponds was deposited and buried in the upstream river, and that the weak tidal currents in the upstream river restricted mixing of SOM sourced from other areas.

Mangroves within the Dongzhai Harbor influenced SOM source contributions near the middle estuary. The proportions of SOM from terrestrial sources were high in the midstream (62.87 %) and upstream (28.30 %) rivers (Fig. 6B), and gradually decreased towards the lower estuary. Additionally, the mean $\delta^{13}\text{C}$ value ($-26.91 \pm 0.40\text{ ‰}$) of the midstream river sediments located near the middle of the estuary fell within the typical range of C3 plants (-29.5 ‰ to -24.4 ‰) (Krishna et al., 2014), and the highest C/N ratio (13.44) was measured in the midstream river near the Dongzhai Harbor Mangrove Reserve. These

results indicate that SOM in surface sediments of the middle estuary likely originated from mangrove forests.

The spatial distribution of SOM derived from marine plankton was nearly opposite the distribution of terrestrial SOM (Fig. 6B). The proportion of plankton-derived SOM was elevated in the DZH main estuary (64.15 %) and downstream river (48.83 %). Additionally, $\delta^{13}\text{C}$ values gradually increased down the land-sea gradient, with more positive values in the lower estuary (Fig. 6A & S1). These trends are consistent with previous studies showing that plankton $\delta^{13}\text{C}$ values in estuaries are a function of salinity and range from -23.9 ‰ to -18 ‰ (Yamamoto, 2000), depending on the source of carbon fixed by phytoplankton (Lamb et al., 2006). The higher levels of plankton-derived SOM in the lower estuary where salinity was higher, were likely related to the long water residence times in the DZH channel. Studies have shown that long water residence times in the DZH channel enhance plankton exposure to sunlight (Xuan et al., 2020). The greater light exposure likely encouraged phytoplankton growth and promoted plankton accumulation on the seafloor in the lower estuary.

4.2. Constraints on SOM preservation and degradation

Estuarine sediments contribute significantly to global biogeochemical cycling of biogenic elements due to the preservation and reactivity of SOM pools in benthic sediments (Keil, 2017; Dan et al., 2019). The SOM pools influence levels of biogenic elements through controls on the sorption/release of nutrients in sediments (Rowley et al., 2017), thus it is important to consider factors that affect SOM preservation and degradation when aiming to develop a better understanding of the role of SOM on mediating coastal chemical budgets.

The PCA analysis in this study revealed positive correlations among TOC, TN, TP, TS, Fe, Mn and clay sediments, while correlations between sand and biogenic elements were negative (Fig. 7A). The correlations are likely owed to the strong effect of sediment grain size on SOM preservation, in which fine sediments provide greater surface area for SOM adsorption (Keith et al., 2014). Thus, the observed correlations indicate that fine-grained sediments enhanced the accumulation and preservation of biogenic elements in the DZH mangrove estuary due to the greater mineral surface area available for organic matter sorption.

The spatial distributions of biogenic elements were similar to the proportion of clay sediments along the estuarine salinity gradient (Fig. 3 & S1). This relationship was related to surface water hydrodynamic

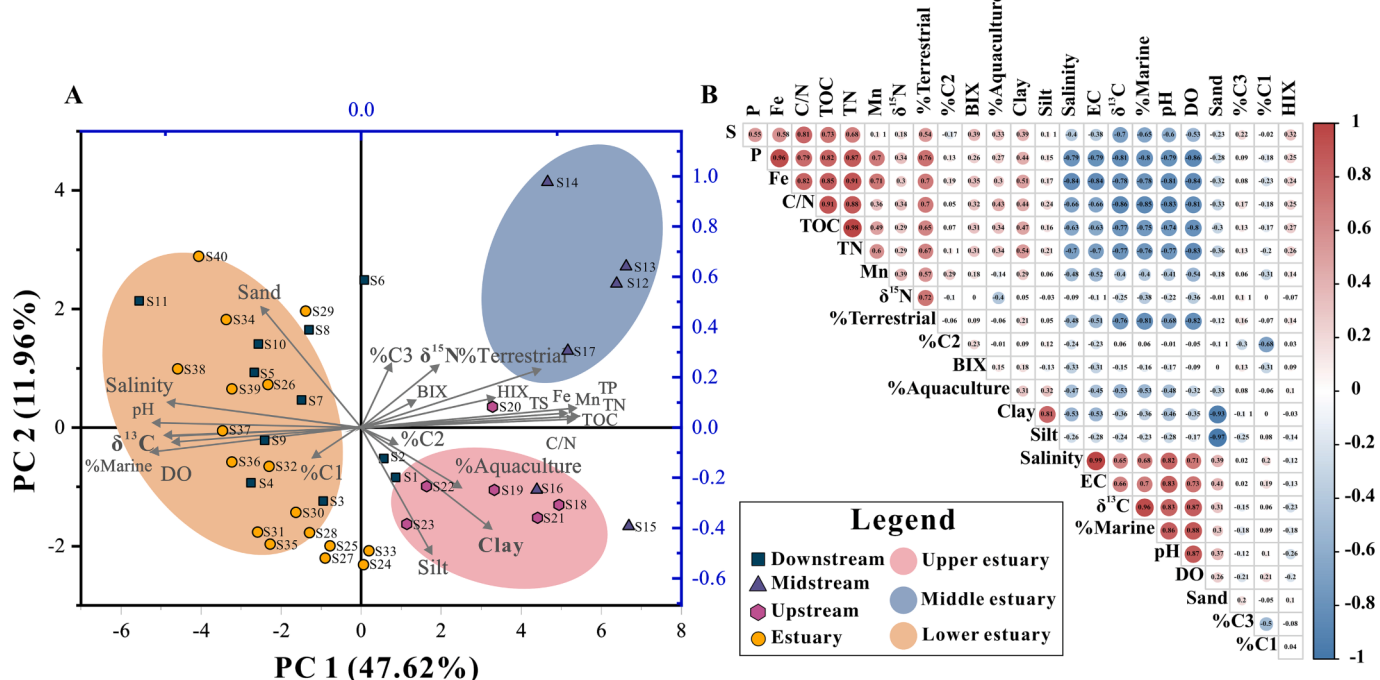


Fig. 7. A) Results of the principal component analysis (PCA). B) PCA correlation matrix for measured (hydro)geochemical parameters. In the PCA matrix, the size and color of the circles represent the correlation coefficient. Blue indicates a positive correlation while red indicates a negative correlation. (For interpretation of the references to color in this figure legend, the reader is referred to the web version of this article.)

patterns. In general, fine benthic sediments such as clays are associated with weak hydrodynamic conditions, while high energy environments are characterized by coarser sediments (Chen et al., 2018). At our study site, coarser sand sediments were clustered in the lower estuary (Fig. 7A). The areas with coarser sediments are higher energy environments with active sediment suspension driven by tides, waves, and currents (Pondell and Canuel, 2017), which limited the burial of SOM. In contrast, weak surface water hydrodynamic forces in the upper estuary promoted SOM deposition and accumulation of biogenic elements.

Aquaculture activity is another factor responsible for SOM preservation. The PCA analysis revealed a cluster of %aquaculture OM and the presence of clay and silt sediments in the upper estuary, as well as a positive correlation between TOC and %aquaculture OM ($r = 0.34$, $p < 0.05$) (Fig. 7A, Table S4). This suggests that weak hydrodynamics in the upper estuary promoted deposition of SOM sourced from aquaculture ponds. The higher SOM deposition was likely due to the influence of aquaculture on increasing sedimentation rates of suspended particles (Pan et al., 2019).

The statistical analysis (Table S4, Fig. 7B) showed a significant positive correlation between TOC, %terrestrial OM, and Fe/Mn. Because organic matter interacts strongly with Fe/Mn minerals, the positive relationships demonstrate that SOM can be preserved as a more stable compound via chelation bonding and coprecipitation with mineral grains (Aftabtalab et al., 2022). Association of SOM-mineral compounds narrows pore spaces and prevents SOM decomposition by catalyzing condensation reactions, altering molecular structure, and inhibiting enzyme access, which can significantly reduce remineralization rates of SOM (Spivak et al., 2019). The stability of such organo-mineral interactions varies with their geochemical composition as well as environmental conditions. For example, in the Yangtze River Estuary, low levels of reactive Fe associated with OM in mobile muds suggested that frequent physical resuspension resulted in desorption, with selective loss of marine SOM (Zhao et al., 2018). Furthermore, humic substances with higher molecular weight and aromaticity can serve as the dominant iron-binding ligands (Krachler and Krachler, 2021). This is likely the case in the DZH estuary, which is supported by the cluster of Fe, Mn,

terrestrial soil-derived fulvic acid C3, and HIX values in the middle estuary (Fig. 7A).

Redox conditions also play a critical role in controlling SOM degradation (Shah Walter et al., 2018). As shown in Fig. 7B, prominently negative relationships were found among DO, TOC, %terrestrial OM, % aquaculture OM, and other biogenic elements, while DO and %marine plankton OM increased up the salinity gradient. Longer exposure of SOM to oxygenated conditions can result in early decomposition and can destroy the SOM-mineral aggregates, further reducing SOM preservation in surface sediments (Arnason and Keil, 2007). Depending on bottom water redox conditions, sediment C/P ratios can vary significantly, with low ratios generally found in oxic conditions and high ratios prevalent in hypoxic or possibly anoxic sediments (Mort et al., 2010). In our study, the significant covariation ($r = 0.97$, $p < 0.001$) between C/P ratios and TOC (Fig. S4) was consistent with anoxic conditions, indicating that anoxia enhanced SOM preservation. The lower C/P ratios of the downstream (average: 20.97) and main estuary (average: 20.96) compared to the upstream (average: 117.05) and midstream (average: 321.30) implied a more oxidizing environment in the lower estuary. Moreover, SOM derived from marine plankton was most labile where strong tidal influences and bioturbation produced more oxic conditions. In such an environment, the plankton-derived SOM would be oxidized more rapidly by the benthic bacterial community (Cook et al., 2007), leading to higher overall SOM degradation rates.

In addition, the seasonal variation may potentially affect SOM dynamics in DZH mangrove estuary. Due to the high riverine discharge, aquaculture-derived OM and terrestrial OM would be higher during the wet season (summer) than dry season (winter). During the rainy season, high temperatures and terrestrial nutrient inputs may promote phytoplankton production, leading to an increase in marine plankton derived SOM. It is possible, however, that low rainfall can result in low river flows/turbidity, and intensive irradiance during the dry season, thereby also favoring phytoplankton growth (Hoffman and Bronk, 2006; Guo et al., 2015). As bottom water temperatures drop in winter, biological productivity decreases, which can further slow down SOM degradation and preserve SOM in mangrove estuarine sediments (Xu et al., 2020).

SOM degradation processes preferentially enrich sediment $\delta^{13}\text{C}$ relative to $\delta^{15}\text{N}$ (Douglas et al., 2022), thus differences between our bulk sediment $\delta^{13}\text{C}$ and $\delta^{15}\text{N}$ values were used to provide insight into the dominant SOM degradation processes in Dongzhai Harbor. The $\delta^{13}\text{C}$ values increased up the salinity gradient and were inversely correlated to C/N ratios, indicating progressive degradation of SOM. During initial diagenesis, Lamb et al. (2006) showed that C/N ratios in the upper and middle estuary of Dongzhai Harbor can increase due to rapid loss of nitrogen. We further observed lower C/N ratios, enriched $\delta^{13}\text{C}$, and higher %marine plankton OM in the lower estuary. These observations indicate that autochthonous (fresh) plankton-derived OM with low molecular weight was preferentially biodegraded during post-depositional processes. Previous studies have shown that these post-depositional processes can preserve NH_3 and release CO_2 or CH_4 as decay products (Dan et al., 2019; Xuan et al., 2019). The spatial trend in average $\delta^{13}\text{C}$ values were generally similar to $\delta^{15}\text{N}$. The average $\delta^{15}\text{N}$ values increased with salinity in sediment samples collected from the upstream river, downstream river, and main estuary (Fig. 2H). This suggests that labile nitrogenous compounds were assimilated during SOM transformation (Denk et al., 2017), which resulted in general enrichment of ^{15}N isotopic signatures in the residual SOM from the upper to lower estuary. However, the highest average $\delta^{15}\text{N}$ value was measured in the midstream river, with a large degree of variability across the individual measurements. The variability was likely due to complex interactions between differences in source contributions and diagenetic alteration under different redox conditions (Canadas et al., 2022).

4.3. Implications for SOM on mangrove wetland environments

The sources, composition, preservation, and degradation processes of SOM as observed in this study have important implications for mangrove growth and development (Fig. 8). Our results show that mangrove litterfall is a key terrestrial source of sedimentary organic matter in certain areas of the Dongzhai Harbor estuary. In turn, SOM entering mangrove wetlands is either produced autochthonously or imported by tides and rivers. In the upper estuary, high proportions of fine-grained sediments and aquaculture-derived biodeposits can facilitate SOM preservation through fine-grained sedimentation. This process is conducive to shoreland accretion and stability, which promotes mangrove forest habitat in face of sea level rise (Krauss et al., 2014).

However, excessive aquaculture-derived OM sequestration beyond ecological balance can transform benthic environments from an oxidized to reduced state in response to heightened microbial processing (Pan et al., 2019). Our results suggest that sediments in the upstream river are likely to shift to reducing conditions, as the upstream river exhibited the highest relative intensity of tryptophan-like (C2) components (average: 11.56 %) sourced from aquaculture. Under such reducing conditions, anaerobic respiration and sulfate reduction can lead to the accumulation of heavy metal sulfides and organic acids (Boye et al., 2017), which could increase the toxicity of the mangrove rhizosphere soil. Additionally, aquaculture ponds surrounding Dongzhai Harbor have elevated nutrient concentrations and SOM levels owing to wastewater discharge, increasing the risk of eutrophication in mangrove wetlands farther down the estuary.

In the middle estuary, most sources of SOM were derived from recalcitrant fine-grained terrestrial organic matter, which has implications for heavy metal phases within mangrove sediments. The PCA analysis revealed a cluster of %terrestrial OM, %C3, HIX, TOC, TN, TP, TS, Fe and Mn (Fig. 7A), indicating adsorption of high molecular weight SOM to biogenic elements (Li et al., 2021). On the one hand, Fe/Mn-humus complexes can associate with heavy metals, thereby reducing heavy metal bioavailability and mobility in sediments (Chen et al., 2020). On the other hand, mangrove plants can release oxygen, oxidize rhizosphere soil, and convert heavy metals into a bioavailable phase, which are absorbed by mangrove roots and transported upward to the aboveground part of the plant (Hu et al., 2021). Mangrove wetlands are limited in the amount of heavy metals they can purify, and when the level of pollution exceeds certain thresholds, the wetland ecosystem is damaged, resulting in reduced plant growth because metabolic processes are adversely affected (Maurya and Kumari, 2021).

In the lower estuary where oxic conditions prevailed, marine plankton-derived bacterial metabolites and by-products were the dominant fraction of SOM. This plankton-derived OM would undergo rapid aerobic degradation due to the large quantity of energy released during oxygen reduction (McDonough et al., 2022). The aerobic respiration rates would be higher in the lower oxygenated estuary compared to the hypoxic upper estuary because anaerobic processes yield lower energy per mole of electron acceptor reduced (Boye et al., 2017). The high degradation potential of SOM in the lower estuary would likely lead to release of inorganic nitrogen, phosphorous, and other biogenic elements to the overlying water column (Schmidt et al., 2011; Zhou

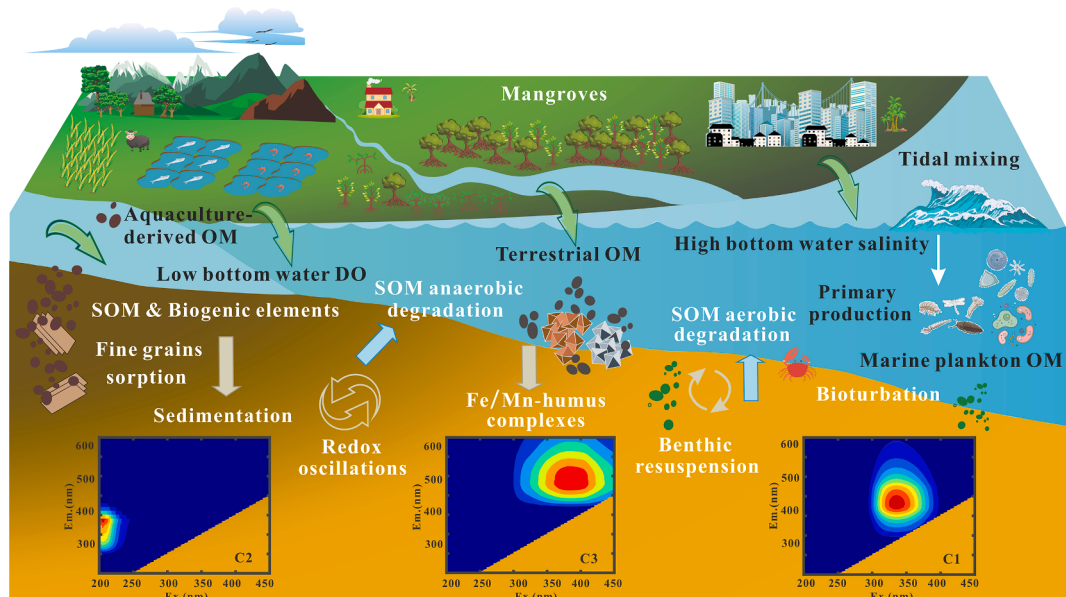


Fig. 8. Conceptual model summarizing the SOM biogeochemical processes impacting mangrove wetland environments in the DZH mangrove estuary.

et al., 2022). The release of these elements from SOM can increase nutrient supply to mangrove forests (Banerjee et al., 2018) and enhance plant growth and survival even under strong tidal and bioturbation effects.

5. Conclusion

This study explored biogeochemical processes impacting sedimentary organic matter (SOM) sources, preservation, and degradation in the Dongzhai Harbor mangrove estuary, where aquaculture activities are extensive. Bulk hydrogeochemistry, carbon and nitrogen isotopes, and optical composition of SOM was characterized at 46 sampling sites along the land-sea estuarine gradient. The measurements showed that biogenic element concentrations (TOC, TN, TP, TS, Fe and Mn) and the proportion of benthic clay particles decreased down the land-sea salinity gradient. A $\delta^{13}\text{C}$ and $\delta^{15}\text{N}$ three-endmember mixing model indicated that SOM was derived primarily from aquaculture, terrestrial sources, and marine plankton in the upper, middle and lower estuary, respectively. Three SOM fluorescent components were identified consisting of a terrestrial/microbial humic-like component (C1), a tryptophan-like component (C2), and a soil-derived fulvic acid (C3). SOM can be preserved through sedimentation due to the high proportion of fine-grained aquaculture-derived biodeposits and weak hydrodynamic conditions in the upper estuary, coupled with formation of Fe/Mn-humus complexes in the middle estuary. The findings also show that microbes can aerobically metabolize SOM sourced from marine plankton in the downstream oxic environment, resulting in faster decomposition of SOM. Additionally, relationships between C/N ratios vs $\delta^{13}\text{C}$ and $\delta^{15}\text{N}$ values indicate progressive SOM degradation, including initial diagenesis and post-depositional processes. These findings provide new insights into the factors that affect SOM dynamics along land-sea transition zones, and have important implications for the environmental sustainability of mangrove estuaries in densely populated regions with aquaculture production.

CRediT authorship contribution statement

Lu Yan: Conceptualization, Investigation, Methodology, Formal analysis, Writing – original draft, Writing – review & editing. **Xianjun Xie:** Conceptualization, Supervision, Funding acquisition. **James W. Heiss:** Writing – original draft, Supervision. **Kang Peng:** Investigation, Methodology. **Yamin Deng:** Project administration, Funding acquisition. **Yiqun Gan:** Project administration. **Qinghua Li:** Funding acquisition. **Yanpeng Zhang:** Resources.

Declaration of Competing Interest

The authors declare that they have no known competing financial interests or personal relationships that could have appeared to influence the work reported in this paper.

Data availability

Data will be made available on request.

Acknowledgements

The research work was financially supported by National Natural Science Foundation of China (42020104005; U2244225), National Key Research and Development Program of China (2021YFA0715900), the Ministry of Education of China (111 project), and the Fundamental Research Funds for the Central Universities, China University of Geosciences (Wuhan) and China Geological Survey (DD20211391). We acknowledge Prof. Xiaoguang Xu for providing support of the Monte Carlo modeling source code. We would like to thank the Associate Editor and reviewers for their valuable contributions that greatly improved this

manuscript.

Appendix A. Supplementary data

Supplementary data to this article can be found online at <https://doi.org/10.1016/j.jhydrol.2023.129256>.

References

- Aftabtalab, A., Rinklebe, J., Shaheen, S.M., Niazi, N.K., Moreno-Jimenez, E., Schaller, J., Knorr, K.H., 2022. Review on the interactions of arsenic, iron (oxy)hydr oxides, and dissolved organic matter in soils, sediments, and groundwater in a ternary system. *Chemosphere* 286 (Pt 2), 131790.
- Alongi, D.M., 2014. Carbon cycling and storage in mangrove forests. *Annu. Rev. Marine Sci.* 6, 195–219.
- Alongi, D.M., 2021. Macro- and micronutrient cycling and crucial linkages to geochemical processes in mangrove ecosystems. *J. Marine Sci. Eng.* 9 (5).
- Andersson, A., 2011. A systematic examination of a random sampling strategy for source apportionment calculations. *Sci. Total Environ.* 412–413, 232–238.
- Arnanson, T.S., Keil, R.G., 2007. Changes in organic matter–mineral interactions for marine sediments with varying oxygen exposure times. *Geochim. Cosmochim. Acta* 71 (14), 3545–3556.
- Ayvazian, S.G., Ray, N.E., Gerber-Williams, A., Grabbert, S., Pimenta, A., Hancock, B., Cobb, D., Strobel, C., Fulweiler, R.W., 2021. Evaluating connections between nitrogen cycling and the macrofauna in native oyster beds in a New England Estuary. *Estuar. Coasts* 45 (1), 196–212.
- Banerjee, K., Bal, G., Mitra, A., 2018. How soil texture affects the organic carbon load in the mangrove ecosystem? A case study from Bhitaranika, Odisha, environmental pollution. *Water Sci. Technol.* Lib. 329–341.
- Bao, H., Wu, Y., Unger, D., Du, J., Herbeck, L.S., Zhang, J., 2013. Impact of the conversion of mangroves into aquaculture ponds on the sedimentary organic matter composition in a tidal flat estuary (Hainan Island, China). *Cont. Shelf Res.* 57, 82–91.
- Bauer, J.E., Cai, W.J., Raymond, P.A., Bianchi, T.S., Hopkinson, C.S., Regnier, P.A., 2013. The changing carbon cycle of the coastal ocean. *Nature* 504 (7478), 61–70.
- Bosch, C., Andersson, A., Krusa, M., Bandh, C., Hovorkova, I., Klanova, J., Knowles, T.D., Pancost, R.D., Evershed, R.P., Gustafsson, O., 2015. Source apportionment of polycyclic aromatic hydrocarbons in Central European Soils with compound-specific triple isotopes ($\delta\text{(13)C}$, $\delta\text{(14)C}$, and $\delta\text{(2)H}$). *Environ. Sci. Technol.* 49 (13), 7657–7665.
- Boye, K., Noël, V., Tfaily, M.M., Bone, S.E., Williams, K.H., Bargar, J.R., Fendorf, S., 2017. Thermodynamically controlled preservation of organic carbon in floodplains. *Nat. Geosci.* 10 (6), 415–419.
- Burdige, D.J., Kline, S.W., Chen, W., 2004. Fluorescent dissolved organic matter in marine sediment pore waters. *Mar. Chem.* 89 (1–4), 289–311.
- Canadas, F., Papineau, D., Leng, M.J., Li, C., 2022. Extensive primary production promoted the recovery of the Ediacaran Shuram excursion. *Nat Commun* 13 (1), 148.
- Chen, C., Hall, S.J., Coward, E., Thompson, A., 2020. Iron-mediated organic matter decomposition in humid soils can counteract protection. *Nat. Commun.* 11 (1), 2255.
- Chen, S., Hong, H., Huang, X., Fang, Q., Yin, K., Wang, C., Zhang, Y., Cheng, L., Algeo, T.J., 2018. The role of organo-clay associations in limiting organic matter decay: Insights from the Dajihu peat soil, central China. *Geoderma* 320, 149–160.
- Chen, M., Hur, J., 2015. Pre-treatments, characteristics, and biogeochemical dynamics of dissolved organic matter in sediments: A review. *Water Res.* 79, 10–25.
- Chen, M., Jaffe, R., 2014. Photo- and bio-reactivity patterns of dissolved organic matter from biomass and soil leachates and surface waters in a subtropical wetland. *Water Res.* 61, 181–190.
- Clark, C.D., Litz, L.P., Grant, S.B., 2008. Saltmarshes as a source of chromophoric dissolved organic matter (CDOM) to Southern California coastal waters. *Limnol. Oceanogr.* 53 (5), 1923–1933.
- Coble, P.G., Del Castillo, C.E., Avril, B., 1998. Distribution and optical properties of CDOM in the Arabian Sea during the 1995 Southwest Monsoon. *Deep Sea Res. Part II: Top. Stud. Oceanogr.* 45 (10–11), 2195–2223.
- Conant, R.T., Ryan, M.G., Agren, G.I., Birge, H.E., Davidson, E.A., Eliasson, P.E., Evans, S.E., Frey, S.D., Giardina, C.P., Hopkins, F.M., Hyvönen, R., Kirschbaum, M.U.F., Lavallee, J.M., Leifeld, J., Parton, W.J., Megan Steinweg, J., Wallenstein, M.D., Martin Wetterstedt, J.Å., Bradford, M.A., 2011. Temperature and soil organic matter decomposition rates - synthesis of current knowledge and a way forward. *Glob. Chang. Biol.* 17 (11), 3392–3404.
- Cook, P.M., Wenzhoefer, F., Glud, R., Janssen, F., Huettel, M., 2007. Benthic solute exchange and carbon mineralization in two shallow subtidal sandy sediments: Effect of advective pore-water exchange. *Limnol. Oceanogr.* 52 (5), 1943–1963.
- Dan, S.F., Liu, S.M., Yang, B., Udoh, E.C., Umoh, U., Ewa-Oboho, I., 2019. Geochemical discrimination of bulk organic matter in surface sediments of the Cross River estuary system and adjacent shelf, South East Nigeria (West Africa). *Sci. Total Environ.* 678, 351–368.
- Dan, S.F., Li, S., Yang, B., Cui, D., Ning, Z., Huang, H., Zhou, J., Yang, J., 2021. Influence of sedimentary organic matter sources on the distribution characteristics and preservation status of organic carbon, nitrogen, phosphorus, and biogenic silica in the Daya Bay, northern South China Sea. *Sci. Total Environ.* 783, 146899.
- Deborde, J., Marchand, C., Molnar, N., Della Patrona, L., Meziane, T., 2015. Concentrations and fractionation of carbon, iron, sulfur, nitrogen and phosphorus in

- mangrove sediments along an intertidal gradient (semi-arid climate, New Caledonia). *J. Marine Sci. Eng.* 3 (1), 52–72.
- Denk, T.R.A., Mohn, J., Decock, C., Lewicka-Szczebak, D., Harris, E., Butterbach-Bahl, K., Kiese, R., Wolf, B., 2017. The nitrogen cycle: A review of isotope effects and isotope modeling approaches. *Soil Biol. Biochem.* 105, 121–137.
- Derrien, M., Brogi, S.R., Goncalves-Araujo, R., 2019. Characterization of aquatic organic matter: Assessment, perspectives and research priorities. *Water Res.* 163, 114908.
- Douglas, P.M.J., Stratigopoulos, E., Park, S., Keenan, B., 2022. Spatial differentiation of sediment organic matter isotopic composition and inferred sources in a temperate forest lake catchment. *Chem. Geol.* 603.
- Du, Y., Deng, Y., Liu, Z., Huang, Y., Zhao, X., Li, Q., Ma, T., Wang, Y., 2021. Novel insights into dissolved organic matter processing pathways in a coastal confined aquifer system with the highest known concentration of geogenic ammonium. *Environ. Sci. Technol.* 55 (21), 14676–14688.
- Fenech, C., Rock, L., Nolan, K., Tobin, J., Morrissey, A., 2012. The potential for a suite of isotope and chemical markers to differentiate sources of nitrate contamination: a review. *Water Res.* 46 (7), 2023–2041.
- Gan, S., Schmidt, F., Heuer, V.B., Goldhammer, T., Witt, M., Hinrichs, K.-U., 2020. Impacts of redox conditions on dissolved organic matter (DOM) quality in marine sediments off the River Rhône, Western Mediterranean Sea. *Geochim. Cosmochim. Acta* 276, 151–169.
- Goñi, M.A., O'Connor, A.E., Kuzyk, Z.Z., Yunker, M.B., Gobeil, C., Macdonald, R.W., 2013. Distribution and sources of organic matter in surface marine sediments across the North American Arctic margin. *J. Geophys. Res. Oceans* 118 (9), 4017–4035.
- Gu, Y.G., Ke, C.L., Liu, Q., Lin, Q., 2016. Polycyclic aromatic hydrocarbons (PAHs) in sediments of Zhelin Bay, the largest mariculture base on the eastern Guangdong coast, South China: Characterization and risk implications. *Mar. Pollut. Bull.* 110 (1), 603–608.
- Gu, Y.G., Ouyang, J., Ning, J.J., Wang, Z.H., 2017. Distribution and sources of organic carbon, nitrogen and their isotopes in surface sediments from the largest mariculture zone of the eastern Guangdong coast, South China. *Marine Pollut. Bull.* 120 (1–2), 286–291.
- Guo, H., Li, X., Xiu, W., He, W., Cao, Y., Zhang, D., Wang, A., 2019. Controls of organic matter bioreactivity on arsenic mobility in shallow aquifers of the Hetao Basin, P.R. China. *J. Hydrol.* 571, 448–459.
- Guo, W., Ye, F., Xu, S., Jia, G., 2015. Seasonal variation in sources and processing of particulate organic carbon in the Pearl River estuary, South China. *Estuar. Coast. Shelf Sci.* 167, 540–548.
- He, Y., Guan, W., Xue, D., Liu, L., Peng, C., Liao, B., Hu, J., Zhu, Q., Yang, Y., Wang, X., Zhou, G., Wu, Z., Chen, H., 2019. Comparison of methane emissions among invasive and native mangrove species in Dongzhaigang, Hainan Island. *Sci. Total Environ.* 697, 133945.
- He, X.S., Xi, B.D., Li, X., Pan, H.W., An, D., Bai, S.G., Li, D., Cui, D.Y., 2013. Fluorescence excitation-emission matrix spectra coupled with parallel factor and regional integration analysis to characterize organic matter humification. *Chemosphere* 93 (9), 2208–2215.
- Hoffman, J.C., Bronk, D.A., 2006. Interannual variation in stable carbon and nitrogen isotope biogeochemistry of the Mattaponi River, Virginia. *Limnol. Oceanogr.* 51 (5), 2319–2332.
- Hu, B., Guo, P., Su, H., Deng, J., Zheng, M., Wang, J., Wu, Y., Jin, Y., 2021. Fraction distribution and bioavailability of soil heavy metals under different planting patterns in mangrove restoration wetlands in Jinjiang, Fujian, China. *Ecol. Eng.* 166.
- Hu, G., Xu, K., Clift, P.D., Zhang, Y., Li, Y., Qiu, J., Kong, X., Bi, S., 2018. Textures, provenances and structures of sediment in the inner shelf south of Shandong Peninsula, western South Yellow Sea. *Estuar. Coast. Shelf Sci.* 212, 153–163.
- Huang, S.B., Wang, Y.X., Ma, T., Tong, L., Wang, Y.Y., Liu, C.R., Zhao, L., 2015. Linking groundwater dissolved organic matter to sedimentary organic matter from a fluvio-lacustrine aquifer at Jianghan Plain, China by EEM-PARAFAC and hydrochemical analyses. *Sci. Total Environ.* 529, 131–139.
- Kappler, A., Bryce, C., Mansor, M., Lueder, U., Byrne, J.M., Swanner, E.D., 2021. An evolving view on biogeochemical cycling of iron. *Nat. Rev. Microbiol.* 19 (6), 360–374.
- Keil, R., 2017. Anthropogenic forcing of carbonate and organic carbon preservation in marine sediments. *Ann. Rev. Mar. Sci.* 9, 151–172.
- Keith, M.K., Sobieszczyk, S., Goldman, J.H., Rounds, S.A., 2014. Investigating organic matter in Fanno Creek, Oregon, Part 2 of 3: Sources, sinks, and transport of organic matter with fine sediment. *J. Hydrol.* 519, 3010–3027.
- Kennedy, M.J., Löhr, S.C., Fraser, S.A., Baruch, E.T., 2014. Direct evidence for organic carbon preservation as clay-organic nanocomposites in a Devonian black shale; from deposition to diagenesis. *Earth Planet. Sci. Lett.* 388, 59–70.
- Kirkby, C.A., Kirkgaard, J.A., Richardson, A.E., Wade, L.J., Blanchard, C., Batten, G., 2011. Stable soil organic matter: A comparison of C:N:P ratios in Australian and other world soils. *Geoderma* 163 (3–4), 197–208.
- Koch, B.P., Souza Filho, P.W.M., Behling, H., Cohen, M.C.L., Kattner, G., Rullkötter, J., Scholz-Böttcher, B., Lara, R.J., 2011. Triterpenols in mangrove sediments as a proxy for organic matter derived from the red mangrove (*Rhizophora mangle*). *Org. Geochem.* 42 (1), 62–73.
- Krachler, R., Krachler, R.F., 2021. Northern High-Latitude Organic Soils As a Vital Source of River-Borne Dissolved Iron to the Ocean. *Environ. Sci. Technol.* 55 (14), 9672–9690.
- Krishna, M.S., Naidu, S.A., Subbaiah, C.V., Gawade, L., Sarma, V.V.S.S., Reddy, N.P.C., 2014. Sources, distribution and preservation of organic matter in a tropical estuary (Godavari, India). *Estuar. Coasts* 38 (3), 1032–1047.
- Lamb, A.L., Wilson, G.P., Leng, M.J., 2006. A review of coastal palaeoclimate and relative sea-level reconstructions using $\delta^{13}\text{C}$ and C/N ratios in organic material. *Earth Sci. Rev.* 75 (1–4), 29–57.
- Li, Z., Li, X., Wang, X., Ma, J., Xu, J., Xu, X., Han, R., Zhou, Y., Yan, X., Wang, G., 2020c. Isotopic evidence revealing spatial heterogeneity for source and composition of sedimentary organic matters in Taihu Lake, China. *Ecol. Indic.* 109.
- Li, H., Xia, Y., Geng, X., 2013. Hydrogeology and hydrochemistry along two transects in mangrove tidal marshes at Dongzhaiyang National Nature Reserve, Hainan, China, groundwater in the coastal zones of Asia-Pacific. *Coast. Res. Library* 11–25.
- Li, H., Santos, F., Butler, K., Herndon, E., 2021. A critical review on the multiple roles of manganese in stabilizing and destabilizing soil organic matter. *Environ. Sci. Tech.* 55 (18), 12136–12152.
- Li, S., Xia, X., Zhang, S., Zhang, L., 2020b. Source identification of suspended and deposited organic matter in an alpine river with elemental, stable isotopic, and molecular proxies. *J. Hydrol.* 590.
- Li, M., Xie, W., Li, P., Yin, K., Zhang, C., 2020a. Establishing a terrestrial proxy based on fluorescent dissolved organic matter from sediment pore waters in the East China Sea. *Water Res.* 182, 116005.
- Liu, Y., Ji, C., Fu, B., He, L., Fu, Q., Shen, M., Zhao, Z., 2019. Factors influencing the accumulation of Pd in mangrove wetland sediments in Dongzhai Harbor, Hainan, China. *J. Coast. Conserv.* 23 (6), 1039–1045.
- Marchand, C., Allenbach, M., Lallier-Vergès, E., 2011. Relationships between heavy metals distribution and organic matter cycling in mangrove sediments (Concept Bay, New Caledonia). *Geoderma* 160 (3–4), 444–456.
- Martinez-Garcia, E., Carlsson, M.S., Sanchez-Jerez, P., Sánchez-Lizaso, J.L., Sanz-Lazaro, C., Holmer, M., 2015. Effect of sediment grain size and bioturbation on decomposition of organic matter from aquaculture. *Biogeochemistry* 125 (1), 133–148.
- Maurya, P., Kumari, R., 2021. Toxic metals distribution, seasonal variations and environmental risk assessment in surficial sediment and mangrove plants (*A. marina*), Gulf of Kachchh (India). *J. Hazard. Mater.* 413, 125345.
- McDonough, L.K., Andersen, M.S., Behnke, M.I., Rutledge, H., Oudone, P., Meredith, K., O'Carroll, D.M., Santos, I.R., Marjo, C.E., Spencer, R.G.M., McKenna, A.M., Baker, A., 2022. A new conceptual framework for the transformation of groundwater dissolved organic matter. *Nat. Commun.* 13 (1), 2153.
- Minu, A., Routh, J., Machiwa, J.F., 2020. Distribution and sources of organic matter in the Rufiji Delta in Tanzania: Variability and environmental implications. *Appl. Geochim.* 122.
- Mort, H.P., Slomp, C.P., Gustafsson, B.G., Andersen, T.J., 2010. Phosphorus recycling and burial in Baltic Sea sediments with contrasting redox conditions. *Geochim. Cosmochim. Acta* 74 (4), 1350–1362.
- Naidu, S.A., Kathiresan, K., Simonson, J.H., Blanchard, A.L., Sanders, C.J., Pérez, A., Post, R.M., Subramonian, T., Naidu, R.A., Narendar, R., 2022. Carbon and nitrogen contents driven by organic matter source within Pichavaram wetland sediments. *J. Marine Sci. Eng.* 10 (1).
- Osburn, C.L., Boyd, T.J., Montgomery, M.T., Bianchi, T.S., Coffin, R.B., Paerl, H.W., 2016. Optical proxies for terrestrial dissolved organic matter in estuaries and coastal waters. *Front. Mar. Sci.* 2.
- Pan, Z., Gao, Q.F., Dong, S.L., Wang, F., Li, H.D., Zhao, K., Jiang, X.Y., 2019. Effects of abalone (*Haliotis discus hannai* Ino) and kelp (*Saccharina japonica*) mariculture on sources, distribution, and preservation of sedimentary organic carbon in Ailian Bay, China. Identified by coupling stable isotopes ($\delta^{13}\text{C}$ and $\delta^{15}\text{N}$) with C/N ratio analyses. *Mar. Pollut. Bull.* 141, 387–397.
- Pondell, C.R., Canuel, E.A., 2017. The role of hydrodynamic sorting on the accumulation and distribution of organic carbon in an impoundment: Englebright Lake, California, USA. *Biogeochemistry* 133 (2), 129–145.
- Prasad, M.B.K., Kumar, A., Ramanathan, A.L., Datta, D.K., 2017. Sources and dynamics of sedimentary organic matter in Sundarban mangrove estuary from Indo-Gangetic delta. *Ecol. Process.* 6 (1).
- Qiao, W., Guo, H., He, C., Shi, Q., Zhao, B., 2021. Unraveling roles of dissolved organic matter in high arsenic groundwater based on molecular and optical signatures. *J. Hazard. Mater.* 406, 124702.
- Resmi, P., Manju, M.N., Gireeshkumar, T.R., Ratheesh Kumar, C.S., Chandramohanakumar, N., 2016. Source characterisation of Sedimentary organic matter in mangrove ecosystems of northern Kerala, India: Inferences from bulk characterisation and hydrocarbon biomarkers. *Reg. Stud. Mar. Sci.* 7, 43–54.
- Rowley, M.C., Grand, S., Verrecchia, É.P., 2017. Calcium-mediated stabilisation of soil organic carbon. *Biogeochemistry* 137 (1–2), 27–49.
- Samantaray, S., Sanyal, P., 2022. Sources and fate of organic matter in a hypersaline lagoon: A study based on stable isotopes from the Pulicat lagoon, India. *Sci. Total Environ.* 807 (Pt 2), 150617.
- Santos, I.R., Chen, X., Lecher, A.L., Sawyer, A.H., Moosdorf, N., Rodellas, V., Tamborski, J., Cho, H.-M., Dimova, N., Sugimoto, R., Bonaglia, S., Li, H., Hajati, M.-C., Li, L., 2021. Submarine groundwater discharge impacts on coastal nutrient biogeochemistry. *Nat. Rev. Earth Environ.* 2 (5), 307–323.
- Sarà, G., Scilipoti, D., Mazzola, A., Modica, A., 2004. Effects of fish farming waste to sedimentary and particulate organic matter in a southern Mediterranean area (Gulf of Castellammare, Sicily): a multiple stable isotope study ($\delta^{13}\text{C}$ and $\delta^{15}\text{N}$). *Aquaculture* 234 (1–4), 199–213.
- Schartup, A.T., Balcom, P.H., Mason, R.P., 2014. Sediment-porewater partitioning, total sulfur, and methylmercury production in estuaries. *Environ. Sci. Tech.* 48 (2), 954–960.
- Schmidt, F., Koch, B.P., Elvert, M., Schmidt, G., Witt, M., Hinrichs, K.-U., 2011. Diagenetic Transformation of dissolved organic nitrogen compounds under contrasting sedimentary redox conditions in the Black Sea. *Environ. Sci. Tech.* 45 (12), 5223–5229.
- Shah Walter, S.R., Jaekel, U., Osterholz, H., Fisher, A.T., Huber, J.A., Pearson, A., Dittmar, T., Girguis, P.R., 2018. Microbial decomposition of marine dissolved organic matter in cool oceanic crust. *Nat. Geosci.* 11 (5), 334–339.

- Spivak, A.C., Sanderman, J., Bowen, J.L., Canuel, E.A., Hopkinson, C.S., 2019. Global-change controls on soil-carbon accumulation and loss in coastal vegetated ecosystems. *Nat. Geosci.* 12 (9), 685–692.
- Stedmon, C.A., Bro, R., 2008. Characterizing dissolved organic matter fluorescence with parallel factor analysis: a tutorial. *Limnol. Oceanogr. Methods* 6 (11), 572–579.
- Tesi, T., Langone, L., Goñi, M.A., Turchetto, M., Misericocchi, S., Boldrin, A., 2008. Source and composition of organic matter in the Bari canyon (Italy): Dense water cascading versus particulate export from the upper ocean. *Deep Sea Res. Part I: Oceanogr. Res. Papers* 55 (7), 813–831.
- Thiri, M., Yang, Y., 2022. Review on Possible Factors for Outbreak of Wood Boring Isopod, *Sphaeroma* spp. Which Causes Destructive Impact on Mangrove Forest in China. *Open J. Ecol.* 12 (03), 211–235.
- Wang, Q., Mei, D., Chen, J., Lin, Y., Liu, J., Lu, H., Yan, C., 2019. Sequestration of heavy metal by glomalin-related soil protein: Implication for water quality improvement in mangrove wetlands. *Water Res.* 148, 142–152.
- Wang, S., Rao, W., Qian, J., Jin, K., Li, K., Feng, Y., Zhao, J., 2021. Sr-Nd isotope and REE compositions of surface sediments from the Three Gorges Reservoir: Implications for source identification and apportionment. *J. Hydrol.*
- Wentworth, C.K., 1922. A scale of grade and class terms for clastic sediments. *J. Geol.* 30 (5), 377–392.
- Xia, D., Vaye, O., Yang, Y., Zhang, H., Sun, Y., 2021. Spatial distributions, source apportionment and ecological risks of C9–C17 chlorinated paraffins in mangrove sediments from Dongzhai Harbor, Hainan Island. *Environ. Pollut.* 270, 116076.
- Xiong, Y., Liao, B., Proffitt, E., Guan, W., Sun, Y., Wang, F., Liu, X., 2018. Soil carbon storage in mangroves is primarily controlled by soil properties: A study at Dongzhai Bay, China. *Sci. Total Environ.* 619–620, 1226–1235.
- Xu, D., Liao, B.W., Zhu, N.H., Guan, W., Li, S.C., Zhong, C.R., 2014. A primary analysis on mangroves degradation in Dongzhaigang of Hainan Island. *Ecol. Sci.* 33, 294–300.
- Xu, C., Yang, B., Dan, S.F., Zhang, D., Liao, R., Lu, D., Li, R., Ning, Z., Peng, S., 2020. Spatiotemporal variations of biogenic elements and sources of sedimentary organic matter in the largest oyster mariculture bay (Maowei Sea), Southwest China. *Sci. Total Environ.* 730, 139056.
- Xuan, Y., Tang, C., Cao, Y., Li, R., Jiang, T., 2019. Isotopic evidence for seasonal and long-term C and N cycling in a subtropical basin of southern China. *J. Hydrol.* 577.
- Xuan, Y., Tang, C., Liu, G., Cao, Y., 2020. Carbon and nitrogen isotopic records of effects of urbanization and hydrology on particulate and sedimentary organic matter in the highly urbanized Pearl River Delta, China. *J. Hydrol.* 591.
- Yamamoto, M., 2000. Chemical tracers of sediment organic matter origins in two coastal lagoons. *J. Mar. Syst.* 26 (2), 127–134.
- Yamashita, Y., Scinto, L.J., Maie, N., Jaffé, R., 2010. Dissolved organic matter characteristics across a subtropical wetland's landscape: application of optical properties in the assessment of environmental dynamics. *Ecosystems* 13 (7), 1006–1019.
- Yan, L., Xie, X., Peng, K., Wang, N., Zhang, Y., Deng, Y., Gan, Y., Li, Q., Zhang, Y., 2021. Sources and compositional characterization of chromophoric dissolved organic matter in a Hainan tropical mangrove-estuary. *J. Hydrol.*, 126572.
- Yang, L., Choi, J.H., Hur, J., 2014. Benthic flux of dissolved organic matter from lake sediment at different redox conditions and the possible effects of biogeochemical processes. *Water Res.* 61, 97–107.
- Zhang, Y., Zhou, L., Zhou, Y., Zhang, L., Yao, X., Shi, K., Jeppesen, E., Yu, Q., Zhu, W., 2021. Chromophoric dissolved organic matter in inland waters: Present knowledge and future challenges. *Sci. Total Environ.* 759, 143550.
- Zhao, B., Yao, P., Bianchi, T.S., Shields, M.R., Cui, X.Q., Zhang, X.W., Huang, X.Y., Schröder, C., Zhao, J., Yu, Z.G., 2018. The role of reactive iron in the preservation of terrestrial organic carbon in estuarine sediments. *J. Geophys. Res. Biogeo.* 123 (12), 3556–3569.
- Zhou, Y., Zhao, C., He, C., Li, P., Wang, Y., Pang, Y., Shi, Q., He, D., 2022. Characterization of dissolved organic matter processing between surface sediment porewater and overlying bottom water in the Yangtze River Estuary. *Water Res.* 215, 118260.
- Zsolnay, Á., 2003. Dissolved organic matter: artefacts, definitions, and functions. *Geoderma* 113 (3–4), 187–209.